Dual-drug amorphous formulation of gliclazide

Marwah Aljohani,[a] Patrick McArdle,[a] and Andrea Erxleben[a,b,*]

[a] School of Chemistry, National University of Ireland, Galway, Ireland

[b] Synthesis and Solid State Pharmaceutical Centre (SSPC), Ireland

*Corresponding author email address: andrea.erxleben@nuigalway.ie

Abstract

Amorphization is a well-established strategy to enhance the dissolution properties of poorly water-soluble drugs. However, the amorphous state is inherently unstable towards recrystallization. Coamorphous systems of a drug and a small-molecule excipient or of two complementary drugs often show an enhanced stability. Diabetes and hypertension are frequently coexistent. In this paper a study on the coamorphization of the poorly water-soluble antidiabetic drug gliclazide (glz) and the antihypertensive drug valsartan (val) is reported. Amorphous glz recrystallized after 1 d under ambient conditions, whereas coamorphous glz-val containing glz and val in a 1:1 or 1:2 molar ratio was stable for at least four months at 20 °C and 56 % relative humidity. The dissolution rate of glz increased in the order crystalline glz < glz-val_1:1 < glz-val_1:2. Furthermore, ternary coamorphous systems of glz, val and an excipient were prepared; glz-val_1:1_PVP, glz-val_1:1_HPC, glz-val_1:1_ALM, glz-val_1:1_MCC (PVP = polyvinylpyrrolidone, HPC = hydroxypropyl cellulose, ALM = α-lactose monohydrate, MCC = microcrystalline cellulose). MCC and HPC did not affect the stability of the coamorphous system, while ALM promoted the recrystallization of glz in glz-val_1:1_ALM during storage and freshly prepared glz-val_1:1_PVP contained small amounts of crystalline glz. Glz-val_1:1_MCC showed enhanced dissolution properties compared to crystalline glz and glz-val_1:1 and is a viable fixed-dose formulation.

Introduction

Coamorphization with a small-molecule coformer is well-documented in the literature as a strategy to enhance the dissolution properties and thus the bioavailability of poorly water-soluble drugs [1-3]. Various types of biocompatible, inactive small-molecule coformers have been successfully studied such as amino acids [4-7], carboxylic acids [8-11], sugars [12], nicotinamide [13], saccharin [14,15], and bile acids [16,17]. The coformer stabilizes the amorphous phase through intermolecular interactions with the drug molecules and/or by providing a physical barrier to recrystallization. In addition to drug-excipient combinations, drug-drug coamorphous systems in which the inactive coformer is replaced by a second complementary drug have been described and highlighted in the literature as a new perspective for fixed-dose combination therapeutics [18,19]. The first dual-drug coamorphous system was reported by Yamamura et al. who showed that coamorphization of cimetidine and naproxen enhanced the stability of the amorphous form of both drugs, resulting in an improved solubility and dissolution rate [20,21]. Lodagekar et al. reported a stable coamorphous system of two antihypertensive drugs, valsartan and cilnidipine. At the therapeutically relevant dose ratio of 16:1 the release of cilnidipine was significantly enhanced [22]. Other examples include the combination of cimetidine and diflunisal [23], indomethacin and naproxen [24], simvastatin and glipizide [25], ritonavir and indomethacin [26], nateglinide and metformin hydrochloride [27], omeprazole and amoxicillin trihydrate [28] and tranilast and diphenhydramine [29].

Coamorphous formulations of two complementary drugs do not only improve patient compliance by reducing the number of medications the patient has to take but may also enhance the therapeutic efficacy through synchronous delivery. Nevertheless, the development of pharmaceutically relevant drug-drug coamorphous systems is challenging. Besides the obvious requirements that the combination must be therapeutically meaningful and that the two drugs form a coamorphous system that is stable towards recrystallization, the dose ratio and frequency and timing of administration must also be compatible with a coamorphous formulation. Generally, coamorphous systems contain the two components in a 1:1 or 1:2 molar ratio as the improved stability over the individual amorphous drugs is attributed to molecular level H bonding interactions.

It is estimated that 40 – 60 % of type 2 diabetes patients have coexistent hypertension with 50%

of adults with diabetes having hypertension at the time of diagnosis [30,31]. The coexistence of hypertension and diabetes has been linked to an increased risk of cardiovascular disease, retinopathy and nephropathy [30]. Gliclazide (glz, Figure 1) is routinely prescribed for the long-term treatment of type II diabetes. Its poor water solubility is responsible for its slow and variable absorption rate and low bioavailability. To develop a glz-antihypertensive coamorphous formulation, we selected valsartan (val, Figure 1) as the antihypertensive. Val is known to be a good glass former due to its high glass transition temperature of around 76 °C [32]. The recommended doses of glz and val are 30 – 120 mg once a day and 80 – 320 mg once a day, respectively. Thus, a 1:1, 1:2 and 2:1 molar ratio would contain appropriate dose combinations of e.g. 75 mg glz/101 mg val, 75 mg glz/202 mg val, and 120 mg glz/80 mg val.

Recently, a limited number of studies on the combination of dual-drug coamorphous systems with excipients have been published. Waikar and Gaud reported a ternary system of nateglinide, metformin hydrochloride and Neusilin®US2 [33]. The silicate was added to improve the flow properties of the coamorphous system. Lenz et al. developed tablet formulations of a coamorphous salt with colloidal silicon dioxide, mannitol (fast dissolving filler), croscarmellose sodium (superdisintegrant) and magnesium stearate (lubricant) [34]. On the other hand, in a small number of studies polymeric excipients have been used to create three-component drug-drug-excipient coamorphous systems with enhanced stability and dissolution properties compared to the respective binary drug-drug combination. Examples are coamorphized flutamide-bicalutamide-poly(methylmethacrylate-co-ethylacrylate), flutamide-bicalutamide-polyvinylpyrrolidone [35], and ezetimibe-simvastatin-kollidon VA65 [36]. Overall, the effect of excipients on coamorphous formulations is an area that has remained largely unexplored.

Here we report a comprehensive study on the coamorphization of glz and val in the absence and in the presence of excipients. We show that glz in coamorphous glz-val has improved dissolution properties compared to crystalline glz and that the dissolution behavior is further enhanced for ternary coamorphous systems containing microcrystalline cellulose or α-lactose monohydrate.

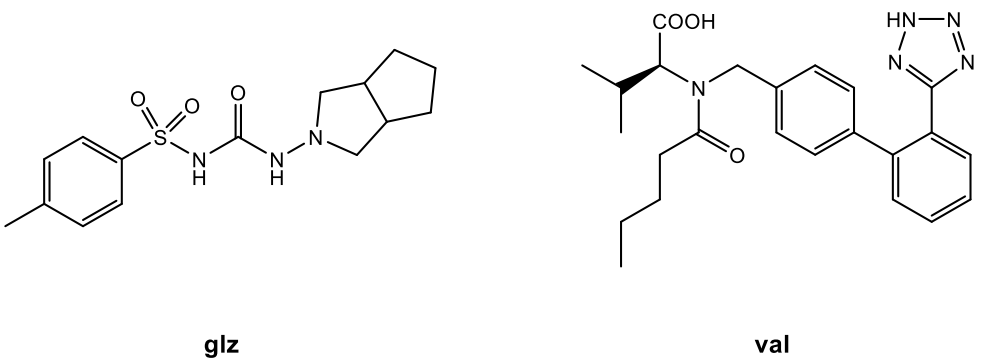

Figure 1. Chemical structures of glz and val.

Materials and methods

Materials

Gliclazide (glz), valsartan (val), polyvinylpyrrolidone (PVP, MW ~10,000, batch #FZZRD-HC) and hydroxypropyl cellulose (HPC, batch #G102-GI$C) were purchased from Tokyo Chemical Industry (TCI Europe). α-Lactose monohydrate (ALM, batch #018K00651) and microcrystalline cellulose (MCC, batch #7130-8C) were supplied by Sigma Aldrich and FMC Biopolymer, respectively.

Methods

Preparation of amorphous glz-val_1:1 and glz-val_1:2

The antidiabetic drug glz and the antihypertensive drug val were physically mixed in a 1:1 and 1:2 molar ratio (0.25 g sample in total). Room temperature milling experiments were performed using an oscillatory ball mill (Mixer Mill MM400, Retsch GmbH & Co., Germany) and a 25 mL stainless steel milling jar containing one 15 mm diameter stainless steel ball. The samples were milled at 25 Hz for 120 minutes with a cool down break of 15 minutes after every 30 minutes of milling. Immediately after milling the powder samples were analyzed by X-ray powder diffraction.

Preparation of amorphous glz-val_2:1

Amorphous glz-val_2:1 was prepared by cryomilling. The milling jars were immersed in liquid

nitrogen for 5 minutes prior to milling and after every 7.5 minutes of milling the jars were cooled again in liquid nitrogen for 2.5 minutes. The milled powder samples were analyzed immediately by X-ray powder diffraction and the amorphous halo appeared after 120 minutes.

Preparation of ternary glz-val-excipient coamorphous systems

The formation of a coamorphous mixture of glz and val in the presence of excipients was investigated. Glz, val and the respective excipient (PVP, MCC, HPC, ALM) were milled together using a glz : val molar ratio of 1:1 and a glz:excipient weight ratio of 1:1 (0.35 g sample in total). The milling experiment was performed at room temperature for 120 min. X-ray powder diffraction analysis was carried out immediately after milling.

X-ray powder diffraction (XRPD)

Coamorphous samples of glz-val_1:1, glz-val_1:2, glz-val_2:1, glz-val_1:1_MCC, glz-val_1:1_HPC, glz-val_1:1_ALM, glz-val_1:1_PVP, glz-MCC (1:1 weight ratio), glz-HPC (1:1 weight ratio), glz-ALM (1:1 weight ratio) and glz_PVP (1:1 weight ratio) were characterized by XRPD immediately after milling. XRPD patterns were recorded between 5 and 90° (2θ) on an Inel Equinox 3000 powder diffractometer using Cu K_α radiation (λ = 1.54178 Å, 35 kV, 25 mA).

FT-IR spectroscopy

FT-IR spectra of freshly prepared samples of coamorphous glz-val_1:1, glz-val_1:2, glz-val_2:1, glz-MCC, glz-HPC, glz-MCC and glz-PVP were collected in the 650 − 3600 cm^{-1} range on a Perkin Elmer Spectrum 400 fitted with an ATR reflectance attachment and a diamond/ZnSe window. The resolution was 4 cm^{-1}.

Differential scanning calorimetry (DSC)

DSC/TGA experiments were performed on freshly prepared samples of coamorphous glz-val_1:1, glz-val_1:2, and glz-val_2:1 with a STA625 thermal analyser (Rheometric Scientific, Piscataway, New Jersey). The runs were performed in open aluminium crucibles between 20 and 300 °C with a heating rate of 10 °C/min. Nitrogen was purged in ambient mode and an indium standard was used for calibration.

Scanning electron microscopy (SEM)

Coamorphous glz-val_1:1, glz-val_1:1_ALM and glz_val_PVP were freshly prepared as described above. Following coating of a thin layer of the respective sample (< 1 mg) with a gold layer to enhance the contrast, the micrograph was captured on a Hitachi S2600N variable pressure scanning electron microscope with the following experimental parameters; ×903 magnification; backscatter BSE resolution of 20 nm at 25 kV, 5 kV accelerating voltage, 10 000 nA emission current, 13.5 mm working distance.

Stability study

To screen the stability of the amorphous materials, the samples were stored in a desiccator at ambient temperature (22 ± 2 ^{o}C) under 56 % and 98 % relative humidity (RH) which was achieved using different concentrations of K_2SO_4 solutions [37]. The stored samples were analyzed after 1, 3, 7, 15, 30, 60 and 120 days by X-ray powder diffraction.

Dissolution study

Dissolution testing was carried out on freshly prepared samples of coamorphous glz-val_1:1, glz-val_1:2, glz-val_2:1, glz-val_1:1_MCC, glz-val_1:1_ALM and cmmercial glz and valsartan All dissolution experiments were performed in triplicate using fresh samples for each run. 100 mg of the respective powder sample was placed in 250 mL 0.1 M phosphate buffer (pH 6.8, 37 °C) and stirred at 300 rpm with an 11-mm magnetic stirring bar. At predetermined time points (2, 5, 10, 15, 25, 30, 45, 60, 90, 120, and 180 minutes) 2.5 mL aliquots were taken and immediately replaced with 2.5 mL of dissolution medium. 50 − 250 μL of the aliquot was diluted by adding 4.95 − 4.75 mL dissolution medium (crystalline glz: 250 μL aliquot/4.75 mL medium; glz-val_1:1, glz-val_1:1_MCC and glz-val_1:1_ALM: 100 μL aliquot/4.90 mL medium; glz-val_1:2: 50 μL aliquot/4.95 mL medium). The amounts of dissolved glz and val were determined on the same day by UV/Vis spectroscopy using a Varian Cary 50 Scan Spectrophotometer (Santa Clara, CA, USA). To exclude any interference from the buffer, reference spectra were recorded for the buffer solution and the buffer solution containing either of the components. Overlapping absorbances of glz and val were treated by measurements at two suitable wavelengths (226 and 240 nm) and simultaneous analysis [38]. Standard solutions (0.0004, 0.0020, 0.0040, 0.0100,

0.0200, 0.0300 and 0.0400 mg/mL) were prepared with phosphate buffer (0.1 M, pH 6.8). The resulting calibration curves were linear in the relevant concentration range.

Results and discussion

Glz and val were mixed in a 1:1, 1:2 and 2:1 molar ratio and ball-milled at room temperature for 2 h. The XRPD patterns of glz-val_1:1 and glz-val_1:2 showed amorphous halos (Figure 2a), while glz-val_2:1 converted to the amorphous state only when the milling was carried out at low temperature (cryomilling, Figure S1). The amorphous samples were characterized by DSC (Figure S2) and FT-IR spectroscopy (Figures S3 – S5). No melting endotherms were visible in the DSC plots of the 1:1 and 1:2 mixture as expected for amorphous solids. The DSC plot of the 2:1 sample showed a recrystallization exotherm at 99.5 °C. The stretching vibration of the C=O group of crystalline glz appears at 1707 cm^{-1}. The ν(C=O) band of the carboxyl group in val is observed at 1729 cm^{-1}. These two bands merge to give a strong, broad band at 1713, 1716 and 1710 cm^{-1} in glz-val_1:1, glz-val_1:2 and glz-val_2:1, respectively. The C=O stretching vibration of the amide group of val and the $\nu_{as}(SO_2)$ vibration of glz that are observed at 1596 and 1346 cm^{-1}, respectively, experience shifts of 3 to 7 wavenumbers in the spectra of the milled samples. The $\nu_{sy}(SO_2)$ band of glz at 1162 cm^{-1} remains unchanged. Overall, the IR data do not suggest strong, specific intermolecular interactions in the coamorphous systems. Examples of coamorphous systems have been reported in the literature that indicate that intimate molecular mixing without the presence of specific intermolecular interactions can stabilize the amorphous phase against recrystallization [17,25]. Lodagekar et al. attributed the formation of stable coamorphous val-cilnidipine in the absence of intermolecular interactions to the antiplasticization effect of val [22].

The stabilities of the coamorphous systems were tested at 20 °C and 56 and 98 % RH (Figures 2, S1 and S6). In all cases the stability was significantly enhanced compared to amorphous glz that is stable for about 1 d at ambient temperature and 56 % RH [39]. At 98 % RH small crystalline peaks of glz were observed in the XRPD pattern of the 1:1 sample after 3 d. In the case of glz-val_1:2 low levels of recrystallized glz were detected after one month under the same conditions. Both samples were stable for at least four months at 20 °C and 56 % RH. Coamorphous gly-

val_2:1 was the least stable with peaks of glz appearing after one month at 56 % RH. None of the XRPD patterns showed Bragg peaks of crystalline val. Guinet et al. have shown that commercial val is of a crystalline mesophase nature in which the long-range order is limited to nano-domains due to frustrated crystallization as a result of conformational disorder [40].

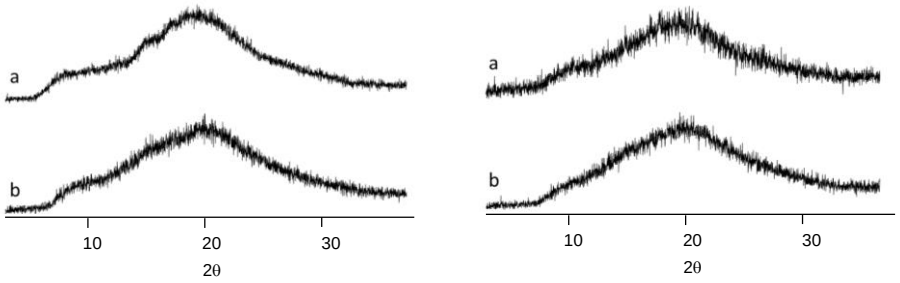

(a) (b)

Figure 2. XRPD patterns of mixtures of glz and val directly after milling for 2 h at room temperature (a) and after milling and storage at 20 °C and 56 % RH for 4 months (b). Top: 1:1 molar ratio. Bottom: 1:2 molar ratio.

Next we investigated the amorphization of glz/val in the presence of common excipients. Glz and val were mixed in a 1:1 molar ratio and microcrystalline cellulose (MCC), hydroxypropyl cellulose (HPC), α-lactose monohydrate (ALM) or polyvinylpyrrolidone (PVP) was added so that the excipient : glz weight ratio was 1:1 (glz-val_1:1_MCC, glz-val_1:1_HPC, glz-val_1:1_ALM and glz-val_1:1_PVP). After milling for 2 h, glz-val_1:1_MCC, glz-val_1:1_HPC and glz-val_1:1_ALM gave amorphous halos (Figures S7 – S9). In the case of glz-val_1:1_PVP small crystalline peaks of glz were observed in the XRPD pattern (Figure S10). PVP is hygroscopic and can absorb significant amounts of water [41]. Water uptake into the sample can facilitate recrystallization and/or prevent amorphization. Amorphous glz-val_1:1_MCC and glz-val_1:1_HPC were stable for at least two months at 20 °C and 56 % RH (Figure S7 and S8). The XRPD pattern of glz-val_1:1_ALM showed peaks of ALM after storage for two weeks at 20 °C and 56 % RH (Figure S9). After two months, small peaks of glz were also visible. In contrast to MCC and HPC, ALM seemed to reduce the stability of amorphous glz in glz-val_1:1_ALM by crystallizing first and then probaly acting as heterogeneous seeds. Freshly prepared samples of

glz-val_1:1_ALM and glz-val_1:1_PVP were examined by SEM and compared with glz-val_1:1 (Figure 3). In all cases the micrographs revealed flat, irregularly-shaped, agglomerated particles with smooth edges and surfaces. The glz-val_1:1 particles were in the 2 – 10 µm range, while the glz-val_1:1_ALM sample showed a greater particle size distribution with a few rather large particles (> 20 µm) being visible. In the micrographs of glz-val_1:1_PVP, small, needle-like crystallites were detected besides the irregularly-shaped amorphous particles.

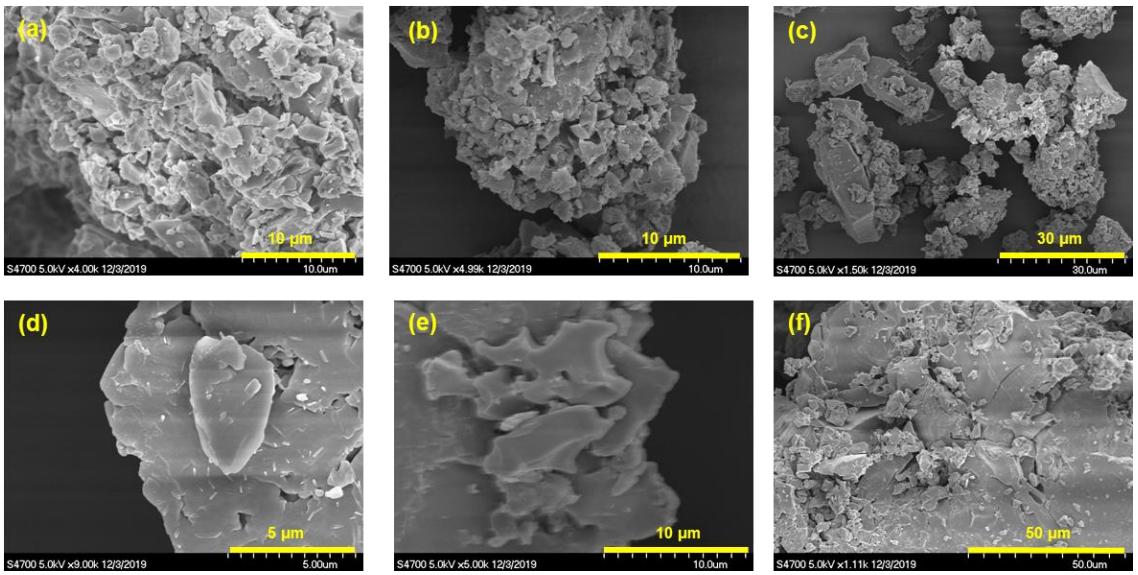

Figure 3. Micrographs of freshly prepared glz-val_1:1 (a), glz-val_1:1_ALM (b and c) and glz_val_PVP (d-f).

It is noteworthy that in the absence of val, binary mixtures of glz with MCC or HPC turned partially amorphous only as indicated by the presence of broadened glz peaks. No shifts of the IR bands of glz were observed (Figure S11). The XRPD pattern of a milled sample of glz and ALM showed broad peaks of the drug and the excipient. Milling with PVP gave an amorphous halo with small glz peaks, similar to the ternary mixture. The N-H and C=O regions of the IR spectrum of the glz/PVP sample did not suggest any specific interactions between glz and PVP (Figure S11).

Figure 4 shows the dissolution profiles of the two stable coamorphous systems, glz-val_1:1 and glz-val_1:2. Glz is released at a faster rate from glz-val_1:1 compared to crystalline glz, although

coamorphous glz-val_1:1 recrystallizes in the dissolution medium (Figure S12). The dissolution rate of glz is further enhanced, when the glz:val ratio in the coamorphous system is 1:2. After 10 min. 56 ± 5 and 79 ± 2 % of glz are released from glz-val_1:1 and glz-val_1:2 respectively, compared to 19 ± 12 % dissolved crystalline glz. Likewise, an increase in the dissolution rate is observed for the ternary systems glz-val_1:1_MCC and glz-val_1:1_ALM compared to glz-val_1:1. As shown in Figures 5 and S13, the release of glz increases in the order crystalline glz < glz-val_1:1 < glz-val_1:1_MCC ~ glz-val_1:1_ALM with about 80 % of glz being released from the ternary systems within 10 min. XRPD analysis shows that in contrast to the binary 1:1 mixture, glz-val_1:1_MCC remains amorphous in the dissolution medium (Figure S14) and this explains the higher dissolution rate of the MCC ternary system. As stated above, there is no evidence for specific molecular interactions between glz and MCC and MCC seems to prevent the recrystallization of the API by acting as a physical barrier. In the case of the ternary system containing ALM, peaks of crystalline glz appear in the XRPD pattern after dissolution testing. Thus, in contrast to glz-val_1:1_MCC, the enhanced dissolution properties of glz-val_1:1_ALM cannot be attributed to the prevention of recrystallization. ALM is readily soluble in water (solubility 195 g L^{-1}) and quantities similar to those in the ternary mixture dissolve instantaneously. The fast dissolution of ALM may facilitate the dissolution of glz-val by ensuring a good dispersibility. Val is released at the same rate from glz-val_1:1 and glz-val_1:2 and there is no significant difference in the absence and in the presence of MCC or ALM.

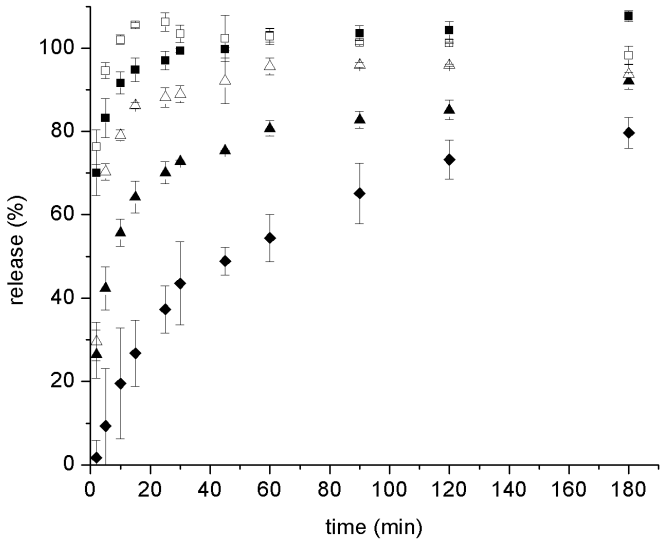

Figure 4. Dissolution profiles of coamorphous glz-val_1:1, coamorphous glz-val_1:2 and crystalline glz. ▲ release of glz from coamorphous glz-val_1:1; Δ release of glz from coamorphous glz-val_1:2; ■ release of val from coamorphous glz-val_1:1; □ release of val from coamorphous glz-val_1:2; ♦ crystalline glz.

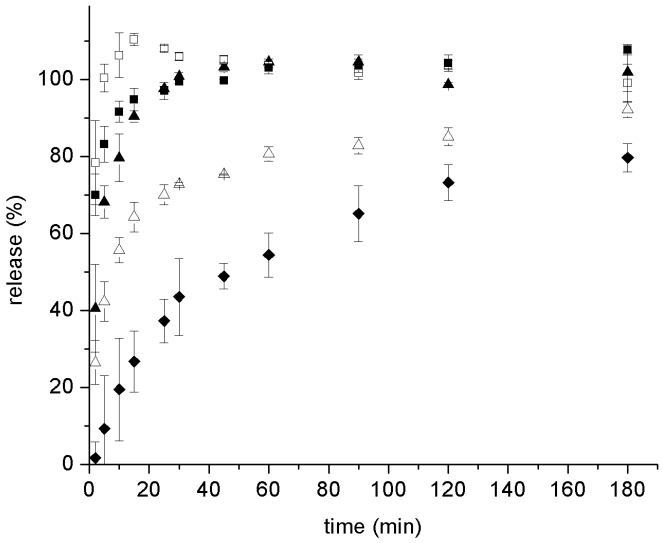

Figure 5. Dissolution profiles of coamorphous glz-val_1:1_MCC (glz : val 1:1 molar ratio, glz : MCC 1:1 weight ratio), coamorphous glz-val_1:1 and crystalline glz. ▲ release of glz from coamorphous glz-val_1:1_MCC; Δ release of glz from coamorphous glz-val_1:1; ■ release of val from coamorphous glz-val_1:1_MCC; □ release of val from coamorphous glz-val_1:1; ♦ crystalline glz.

Conclusions

The complementary drugs glz and val form a stable coamorphous system with enhanced dissolution properties, when mixed in a pharmaceutically relevant ratio. The excipient ALM further improves the dissolution rate of glz, but reduces the stability of the amorphous phase. By contrast, the ternary coamorphous mixture of glz, val and MCC is stable towards crystallization, both during storage and during dissolution testing.

Acknowledgement

This publication has emanated from research supported in part by a research grant from Science Foundation Ireland (SFI) and is cofunded under the European Regional Development Fund under Grant Number 12/RC/2275. M.A. acknowledges the Royal Embassy of Saudi Arabia for a Saudi Arabia Government Scholarship.

Declaration of interest

The authors report no declaration of interest.

References

[1] Newman A, Reutzel-Edens SM, Zografi G. Coamorphous active pharmaceutical ingredient-small molecule mixtures: considerations in the choice of coformers for enhancing dissolution and oral bioavailability. J Pharm Sci 2018;107:5–17.

[2] Laitinen R, Löbmann K, Grohganz H, Priemel P, Strachan CJ, Rades T. Supersaturating drug delivery systems: the potential of co-amorphous drug formulations. Int J Pharm 2017;532:1–12.

[3] Grohganz H, Priemel PA, Löbmann K, Nielsen LH, Laitinen R, Mullertz A, Van den Mooter G, Rades T. Refining stability and dissolution rate of amorphous drug formulations. Expert Opin Drug Deliv 2014;11:977–989.

[4] Jensen KT, Löbmann K, Rades T, Grohganz H. Improving co-amorphous drug formulations by the addition of the highly water soluble amino acid proline. Pharmaceutics 2014; 6:416–435.

[5] Löbmann K, Grohganz H, Laitinen R, Strachan C, Rades T. Amino acids as co-amorphous stabilizers for poorly water soluble drugs-Part 1: Preparation, stability and dissolution enhancement. Eur J Pharm Biopharm 2013;85:873–881.

[6] Laitinen R, Löbmann K, Grohganz H, Strachan C, Rades T. Amino acids as co-amorphous excipients for simvastatin and glibenclamide: physical properties and stability. Mol Pharm 2014;11:2381–2389.

[7] Jensen KT, Blaabjerg LI, Lenz E, Bohr A, Grohganz H, Kleinebudde P, Rades T, Löbmann K. Preparation and characterization of spray-dried co-amorphous drug–amino acid salts. J Pharm Pharmacol 2016;68:615–624.

[8] Lu Q, Zografi G. Phase behavior of binary and ternary amorphous mixtures containing indomethacin, citric acid, and PVP. Pharm Res 1998;15:1202–1206.

[9] Hoppu P, Jouppila K, Rantanen J, Schantz S, Juppo AM. Characterisation of blends of paracetamol and citric acid. J Pharm Pharmacol 2007;59:373–382.

[10] Ali AMA, Ali AA, Maghrabi IA. Clozapine-carboxylic acid plasticized co-amorphous dispersions: preparation, characterization and solution stability evaluation. Acta Pharm 2015;65:133–146.

[11] Han Y, Pan Y, Lv J, Guo W, Wang J. Powder grinding preparation of co-amorphous β-azelnidipine and maleic acid combination: molecular interactions and physicochemical properties. Powder Technol 2016;291:110–120.

[12] Teja A, Musmade PB, Khade AB, Dengale SJ. Simultaneous improvement of solubility and permeability by fabricating binary glassy materials of Talinolol with Naringin: solid state characterization, in-vivo in-situ evaluation. Eur J Pharm Sci 2015;78:234–244.

[13] Shayanfar A, Ghavimi H, Hamishekar H, Jouyban A. Coamorphous atorvastatin calcium to improve its physicochemical and pharmacokinetic properties. J Pharm Pharm Sci 2013;16:577–587.

[14] Qian S, Heng S, Wei Y. Co-amorphous lurasidone hydrochloride-saccharin with charge-assisted hydrogen bonding interaction shows improved physical stability and enhanced dissolution with pH-independent solubility behavior. Cryst Growth Des 2015;15:2920–2928.

[15] Gao Y, Liao J, Qi X, Zhang J. Coamorphous repaglinide–saccharin with enhanced dissolution. Int J Pharm 2013;450:290–295.

[16] Gniado K, Löbmann K, Rades T, Erxleben A. The influence of co-formers on the dissolution rates of co-amorphous sulfamerazine/excipient systems. Int J Pharm 2016;504:20–26.

[17] Gniado K, MacFhionnghaile P, McArdle P, Erxleben A. The natural bile acid surfactant sodium taurocholate (NaTC) as a coformer in coamorphous systems: enhanced physical stability and dissolution behavior of coamorphous drug-NaTC systems. Int J Pharm 2017;535:132–139.

[18] Laitinen R, Löbmann K, Strachan CJ, Grohganz H, Rades T. Emerging trends in the stabilization of amorphous drugs. Int J Pharm 2013;453:65–79.

[19] Chavan RB, Thipparaboina R, Kumar D, Shastri NR. Co amorphous systems: a product development perspective. Int J Pharm 2016;515:403–415.

[20] Yamamura S, Momose Y, Takahashi K, Nagatani S. Solid-state interaction between cimetidine and naproxen. Drug Stab 1996;1:173–178.

[21] Yamamura S, Gotoh H, Sakamoto Y, Momose Y. Physicochemical properties of amorphous precipitates of cimetidine–indomethacin binary system. Eur J Pharm Biopharm 2000;49:259265.

[22] Lodagekar A, Chavan RB, Chella N, Shastri NR. Role of valsartan as an antiplasticizer in development of therapeutically viable drug−drug coamorphous system. Cryst Growth Des 2018;18:1944–1950.

[23] Yamamura S, Gotoh H, Sakamoto Y, Momose Y. Physicochemical properties of amorphous salt of cimetidine and diflunisal system. Int J Pharm 2002;241:213–221.

[24] Löbmann K, Laitinen R, Grohganz H, Gordon KC, Strachan C, Rades T. Coamorphous drug systems: enhanced physical stability and dissolution rate of indomethacin and naproxen. Mol Pharm 2011;8:1919–1928.

[25] Löbmann K, Strachan C, Grohganz H, Rades T, Korhonen O, Laitinen R. Co-amorphous simvastatin and glipizide combinations show improved physical stability without evidence of intermolecular interactions. Eur J Pharm Biopharm 2012;81:159–169.

[26] Dengale SJ, Ranjan OP, Hussen SS, Krishna B, Musmade PB, Shenoy GG, Bhat K. Preparation and characterization of co-amorphous Ritonavir–Indomethacin systems by solvent

evaporation technique: improved dissolution behavior and physical stability without evidence of intermolecular interactions. Eur J Pharm Sci 2014;62:57–64.

[27] Wairkar S, Gaud R. Co-amorphous combination of nateglinide-metformin hydrochloride for dissolution enhancement. AAPS PharmSciTech 2015;17:1–9.

[28] Russo MG, Sancho MI, Silva LM, Baldoni HA, Venancio T, Ellena J, Narda GE. Looking for the interactions between omeprazole and amoxicillin in a disordered phase. An experimental and theoretical study. Spectrochim Acta A Mol Biomol Spectrosc 2016;156:70–77.

[29] Ueda H, Kadota K, Imono M, Ito T, Kunita A, Tozuka Y. Co-amorphous formation induced by combination of tranilast and diphenhydramine hydrochloride. J Pharm Sci 2017;106:123–128.

[30] Sowers JR, Epstein M, Frohlich ED. Diabetes, hypertension, and cardiovascular disease: An update. Hypertension 2001;37:1053–1059.

[31] Klein R, Klein BEK, Lee KE, Cruickshanks KJ, Moss SE. The incidence of hypertension in insulin-dependent diabetes. Arch Intern Med 1996;156:622–627.

[32] Skotnicki M, Gaweł A, Cebe P, Pyda M. Thermal behavior and phase identification of Valsartan by standard and temperature-modulated differential scanning calorimetry. Drug Dev Ind Pharm 2013;39:1508–1514.

[33] Wairkar S, Gaud R. Development and characterization of microstructured, spray-dried co-amorphous mixture of antidiabetic agents stabilized by silicate. AAPS PharmSciTech 2019;20:141.

[34] Lenz E, Jensen KT, Blaabjerg LI, Knopa K, Grohganz H, Löbmann K, Rades T, Kleinebudde P. Solid-state properties and dissolution behaviour of tablets containing co-amorphous indomethacin–arginine. Eur J Pharm Biopharm 2015;96:44–52.

[35] Pacult J, Rams-Baron M, Chmiel K, Jurkiewicz K, Antosik A, Szafraniecc J, Kurek M, Jachowicz R, Paluch M. How can we improve the physical stability of co-amorphous system containing flutamide and bicalutamide? The case of ternary amorphous solid dispersions. Eur J Pharm Sci 2019;136:104947.

[36] Knapik-Kowalczuk J, Chmiel K, Jurkiewicz K, Correia NT, Sawicki W, Paluch M. Physical stability and viscoelastic properties of co-amorphous ezetimibe/simvastatin system. Pharmaceuticals 2019;12:40.

[37] Lu T, Chen C. Uncertainty evaluation of humidity sensors calibrated by saturated salt solutions. Measurement 2007;40:591–599.

[38] Sawyer DT, Heineman WR, Beebe, JM, 1984. Chemistry Experiments for Instrumental Methods. John Wiley & Sons.

[39] Aljohani M, MacFhionnghale P, McArdle P, Erxleben A. Investigation of the formation of drug-drug cocrystals and coamorphous systems of the antidiabetic drug gliclazide. Int J Pharm 2019;561:35–42.

[40] Guinet Y, Paccou L, Danède L, Derollez P, Hédoux A. Structural description of the marketed form of valsartan: A crystalline mesophase characterized by nano crystals and conformational disorder. Int J Pharm 2017;526:209–216.

[41] Fitzpatrick S, McCabe JF, Petts CR, Booth SW. Effect of moisture on polyvinylpyrrolidone in accelerated stability testing. Int J Pharm 2002;246:143–151.